coatings

Article

Study on Rheological Properties of Nano Titanium Dioxide High-Viscosity Modified Asphalt

Ruiduo Li [1,2], Yanzhao Yuan [1], Yabing Ma [1], Zhigang Wang [3], Shikang Zhou [4] and Liqin Li [5,6,*]

[1] School of Civil and Transportation Engineering, Henan University of Urban Construction, Pingdingshan 467036, China; lird@huuc.edu.cn (R.L.); yyz@huuc.edu.com (Y.Y.); xiaomabing@126.com (Y.M.)
[2] Henan Key Laboratory of Engineering Materials and Hydraulic Structures, Zhengzhou University, Zhengzhou 450001, China
[3] Pingdingshan Highway Development Center, Pingdingshan 4467036, China; kldyy@163.com
[4] China Communications First Highway Group Xiamen Engineering Co., Ltd., Xiamen 361000, China; kzhoucqjt@163.com
[5] School of Life Sciences and Engineering, Henan University of Urban Construction, Pingdingshan 467036, China
[6] College of Materials Science and Engineering, Xi'an University of Architecture and Technology, Xi'an 710055, China
* Correspondence: liliqin117@126.com

Abstract: The research on nano titanium dioxide (nano-TiO_2)-modified asphalt has received increasing attention. However, further studies are required in order to ascertain the influence of the phenomenon under discussion on the rheological characteristics and ability to resist deformation of bitumen. In the present study, modified bitumen was formulated by adding nano titanium dioxide. Physical property tests, temperature scanning tests, frequency scanning tests, repeated creep recovery tests, bending creep stiffness tests, and long-term aging performance experiments were carried out on the specimen of asphalt that had undergone the process of modification in order to assess the rheological characteristics and ability to resist unrecoverable deformation of the modified bitumen at different temperatures, both high and low. The outcomes of the repeated creep recovery experiment were analyzed using Burgers and fractional derivative models. The microstructure of nano-TiO_2 high-viscosity modified asphalt was observed by Scanning Electron Microscope(SEM). In order to ascertain the manner in which base bitumen and nano-TiO_2 interact, Fourier transform infrared spectroscopy (FTIR) was utilized in the study. The results show that the thermal stability and prolonged aging resistant properties of the modified bitumen binder improved, but nano-TiO_2 made the asphalt binder weaker and more likely to crack at lower temperatures. Taking into account the variation in the road performance of the bitumen binder, 6% is recommended as the optimal amount of nano-TiO_2. Nano-TiO_2 was mainly uniformly distributed in asphalt and nano-TiO_2 was physically mixed with asphalt. In comparison with the Burgers model, the present fractional derivative empirical creep model can fit the creep test data of the asphalt binder well with the advantages of high accuracy and few parameters. The research results provide a reference for promoting the implementation of modified bitumen incorporating nano-TiO_2.

Keywords: nano-TiO_2; rheological property; Burgers model; fractional derivative empirical creep model

check for updates

Academic Editor: Claudio Lantieri

Received: 19 May 2025
Revised: 6 June 2025
Accepted: 11 June 2025
Published: 14 June 2025

Citation: Li, R.; Yuan, Y.; Ma, Y.; Wang, Z.; Zhou, S.; Li, L. Study on Rheological Properties of Nano Titanium Dioxide High-Viscosity Modified Asphalt. *Coatings* **2025**, *15*, 717. https://doi.org/10.3390/coatings15060717

Copyright: © 2025 by the authors. Licensee MDPI, Basel, Switzerland. This article is an open access article distributed under the terms and conditions of the Creative Commons Attribution (CC BY) license (https://creativecommons.org/licenses/by/4.0/).

1. Introduction

With the expansion of the urban scale, many negative problems have arisen, such as traffic congestion, air pollution, rising temperatures, etc., which have had adverse effects

on humans. Among them, the urban temperature increase caused by the heat island effect is especially severe. Research shows that the annual average temperature inside the city is at least 2 °C higher than that in the outer suburbs, and in hot summer, there exists a 10 °C temperature difference between indoors and outdoors [1–4].

Urban road paving is an important cause of the heat island problem. Especially during the summer months, the ambient temperature is even more than 20 °C lower than that of asphalt pavements. Under such high environmental temperatures, asphalt pavements often suffer from oil immersion, tire sticking, and rutting under the continuous action of vehicle loads. These diseases will seriously reduce the performance and service life of asphalt roads. To reduce asphalt pavement diseases, scientists use different modifiers to improve the different properties of base asphalt. For polymer modifiers, styrenebutadiene styrene builds a network structure with asphalt by absorbing low molecular asphalt [5]. Styrene butadiene rubber makes asphalt more ductile and increases the fracture resistance of asphalt at low temperatures [6]. Polyethylene could be used to enhance the good fatigue resistance of asphalt [7]. In the context of nanomaterials, the presence of nano-TiO_2 particles has been demonstrated to have a significant impact on the photooxidation behavior of bitumen. Specifically, the incorporation of nano-TiO_2 into modified bitumen has been shown to enhance resistance to photooxidation senescence [8]. The nano-zinc oxide could decrease the irrecoverable strain of hot mix asphalt (HMA) paving [9].

Nano-TiO_2 is a photoactive nanoparticle and an environmentally friendly green material. It was confirmed that titanium dioxide reduced the nitrogen dioxide and sulfur dioxide produced by vehicles in a road environment through its photocatalytic effect to purify the air [10]. Due to its non-toxic and inexpensive, nano-TiO_2 has also been used in road pavements to reduce road temperature and slow down asphalt aging in recent years [11,12]. Many studies have focused on the influence of varying doses of nano-TiO_2 on the physical and rheological characteristics, rutting, prolonged and short-term aging characteristics of bitumen [13,14]. Chen et al. conducted a study on the characteristics of 2% TiO_2 and the organic montmorillonite compound-modified bitumen. The findings demonstrated that the thermal characteristics, ability to resist unrecoverable deformation, thermal oxidation, and resistance to ultraviolet oxidative aging of asphalt were improved [15]. Ji et al. conducted a study on the behavior of modified bitumen with varying characteristics of thermoplastic polyurethane and TiO_2, ranging from 1% to 3% of the total mixture. The results indicated the thermal resistance to oxygen and ability to resist unrecoverable deformation of TiO_2-modified bitumen [16]. Lima et al. modified bitumen using SBS and TiO_2 (0.1%, 0.25% and 0.5%). They investigated the ability to resist the aging impact on bitumen, which was found to decrease over time due to the presence of a carbonyl group [17]. Zheng et al. conducted a study on the performance of asphalt in the presence of titanium dioxide, with concentrations ranging from 2% to 4%. The results indicated that there was an enhancement in resistance to unrecoverable deformation and cracking. The UV aging resistance was improved [8].

These studies provide important technical support for the application of nanosized titanium dioxide. From the above research, it is clear that nano titanium dioxide can improve the aged properties and rheological characteristics of bitumen under small nano-TiO_2 contents. However, further in-depth research is required to ascertain whether the incorporation of large amounts of titanium dioxide exerts a favorable impact on the aging performance and rheological characteristics of bitumen. In addition, there is a lack of necessary research on the viscoelastic deformation characteristics and constitutive model of nano-TiO_2-modified asphalt under a high titanium dioxide content, which is also an important basis for analyzing the deformation characteristics of bitumen binders.

The objective and scope of the research are to explore in-depth the rheological properties and deformation resistance under high temperatures of nano-TiO_2-modified asphalt by physical property tests, temperature scanning tests, frequency scanning tests, repeated creep recovery tests, and bending creep stiffness tests. The Burgers model and the fractional derivative empirical creep equation were utilized to evaluate the experimental outcomes. The microstructure of nano-TiO_2-modified bitumen was observed by SEM. The interplay between base bitumen and nano-TiO_2 was investigated through the utilization of FTIR. The results show that the heightened temperature tolerance of NHV-modified bitumen, augmented with nano-TiO_2, has been enhanced. Nano-TiO_2 has been demonstrated to have a substantial impact on the thermal stability of bitumen at heightened temperatures. Moreover, the incorporation of nano-TiO_2 can reduce their sensitivity and improve the elastic properties of the asphalt binder. The ability to resist rutting has been enhanced, but the resistance to cold-weather cracking has decreased. Taking into account the variation in road performance of nano-TiO_2 high-viscosity modified asphalt with the amount of nano-TiO_2, 6% is recommended as the optimal amount of nano-TiO_2. The fractional derivative empirical creep (FDEC) model offers a superior reflection of the creep properties of modified bitumen and has the advantages of fewer parameters and high precision.

2. Materials and Methods

2.1. Materials

2.1.1. Base Asphalt

The original bitumen with a penetration grade of 60/80 was provided by Alpha (Jiangyin) Asphalt Company, a Chinese enterprise, Jiangyin, China.

2.1.2. BW-HPM High-Viscosity Modifier

BW-HPM high-viscosity asphalt modifier (as shown in Figure 1a), mainly composed of polymers, was used. BW-HPM can effectively increase the viscosity and strengthen asphalt, and enhance the anti-aging properties, durability, and crack resistance of asphalt pavement. BW-HPM was developed by Xi'an Bowang New Materials Technology Co., Ltd, Xi'an, China.



(**a**) (**b**)

Figure 1. (**a**) BW-HPM high adhesive; (**b**) nano-TiO_2.

2.1.3. Nano-TiO_2

The nano-TiO_2 modifier (Figure 1b) employed in our study was supplied by Jinan Zhiding Welding Materials Company, Jinan, China. Nano-TiO_2 is often used as a functional filler or additive, which can enhance the physical characteristics, thermal stability, light stability, and other characteristics of bitumen binder. Its main performance indica-

tors are set out in Table 1. The quantities of nano titanium dioxide are 0%, 3%, 6%, and 9%, correspondingly.

Table 1. The primary technical indicators of nano titanium dioxide.

	Average Size (nm)	Purity (%)	Specific Surface Area (m^2/g)	Bulk Density (g/cm^3)	Density (g/cm^3)
Nano-TiO_2	20	99.9	70–90	0.22	3.9

2.1.4. Preparation of Nano-TiO_2-Modified Asphalt

First, the road 70 petroleum asphalt was placed in the oven for more than 4 h (the set oven temperature was 140 °C ± 10 °C), and then it was taken out and heated in the electric furnace at a temperature of 170 °C ± 10 °C. According to the manufacturer's suggestion, 9% high viscosity agent was added and high-speed shear emulsifier(Fluko-A25, Shanghai Furuk Technology Development Co., Ltd, Shanghai, China) was used to at a 2000 r/min rate for 30 min. Then, we prepared 0%, 3%, 6%, and 9% nano-TiO_2 high-viscosity modified asphalt according to the above steps.

2.2. Experimental Methods

The methodological framework is shown in Figure 2. The parameters designed in all experiments are shown in Sections 2.2.1–2.2.8.

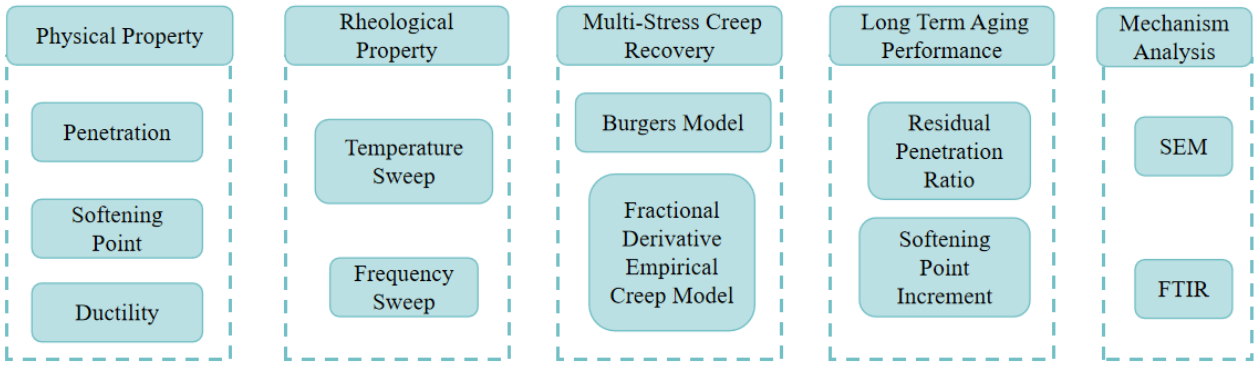


Figure 2. Methodological framework.

2.2.1. Physical Property Tests

The physical property tests were carried out as stipulated in T0604, T0606, and T0605 in the specification JTG E20-2011 [18]. The physical characteristic tests of nano-TiO_2 high-viscosity modified asphalt were conducted, involving penetration, softening point and ductility tests. The temperature in the penetration tests was set to 25 °C. The temperature in the ductility tests was set at 15 °C with a rate of loading of 50 mm/min. The softening point experiments were performed using the Ring and Ball method.

2.2.2. Temperature Sweep Test

In our study, we conducted a series of temperature sweep tests to evaluate the rheological characteristics of the nano-TiO_2 high-viscosity modified asphalt. The performance index of the modified asphalt binder, including complex shear modulus (G*) and phase angle (δ), was acquired through the utilization of the DHR-1 dynamic shear rheometer. The temperature sweeping experiment was performed at a range of temperatures from 34 °C to 82 °C, with a 6 °C increment and a constant angular velocity of 10 rad/s. The parallel metal plates were as follows: 25 mm in terms of diameter, and 1 mm in terms of gap. The

rheological behaviors of the modified bitumen binder at elevated and low temperatures were assessed using the rutting factor obtained through experiments [19].

2.2.3. Frequency Sweep Test

The frequency sweeping experiments conducted involved a scope of 1–100 rad/s at temperatures ranging from 30 °C to 60 °C with an interval of 10 °C. Then, the frequency scanning curve of the bitumen binder was matched and evaluated by employing a straight line equation [20].

2.2.4. Multi-Stress Creep Recovery (MSCR) Test

The DSR instrument was utilized to load asphalt for 1 s and unload asphalt for 9 s under stress of 25 Pa, and the cycle was repeated 60 times within the temperature region of 30 °C–60 °C with an interval of 10 °C. The MSCR test was conducted with the aid of the TA DHR-1 apparatus. The 25 mm parallel plate with a 1 mm gap was selected. Then, the results of the creep recovery test were systematically fitted and analyzed by using the Burgers model of viscoelasticity theory and the fractional derivative empirical creep (FDEC) model [21,22].

2.2.5. Bending Creep Stiffness Test

The creep behavior of pitch under low-temperature conditions was determined by a constant load and by measuring the bending deformation of girder specimens at low temperatures (such as −6 °C, −12 °C and −18 °C). Then, the creep parameters, namely the stiffness, S (t), and the rate, m (t) [23], were computed. The value of the bending creep stiffening and m-value of the bitumen binder were determined by the implementation of a bending beam rheometer. The test temperature conditions were −6 °C, −12 °C, and 18 °C, respectively.

2.2.6. Long-Term Aging Performance Test

As stated in JTG E20-2011 [18], the prolonged aging characteristics of bituminous specimens were tested using a pressure aging oven. The asphalt sample after thermal-oxidative aging treatment was loaded into a sample tray. The container pressure was 2.1 MPa. At 100 °C, the asphalt sample was continuously aged for 20 h, and the prolonged aging of the bituminous specimens was completed. The penetration index and softening point index were conducted following prolonged aging. The material's behavior when aged was evaluated by calculating its residual penetration ratio and softening point increment.

2.2.7. Scanning Electron Microscope (SEM) Test

Scanning electron microscopy (Quanta 450, FEI, Waltham, MA, USA) was employed to observe the microstructure of asphalt specimen. The asphalt sample was gold-plated due to its weak conductivity. The spraying voltage was 10 mA. The spraying target material was gold–palladium alloy. The spraying time was 45 s. The dried asphalt sample was uniformly pasted onto the conductive adhesive for testing.

2.2.8. Fourier Transform Infrared Spectroscopy (FTIR) Test

The surface functional groups of bitumen were analyzed by Fourier transform infrared spectroscopy (Nicolet iS10, Waltham, MA, USA). Next, 1 mg of asphalt samples and 200 mg of dried KBr were thoroughly mixed and ground. The mixture was evenly placed between the top and bottom molds of the tablet mold. The pressure was set to 8 t/cm^2 and the pressurization time was 2 min. The transparent sample ingot was prepared. The sample diameter was 13 mm and the thickness was 1 mm. The sample ingot was placed in the instrument. The spectral range was 500–4000 cm^{-1}.

3. Results and Discussion

3.1. Physical Property

The physical characteristics of the prepared bitumen binder are shown in Figure 3. From Figure 3, it can be seen that with the rising percentage of nanoscale titanium dioxide, the penetration index of the bitumen binder and its ductility undergo a gradual decrease, while its softening point increases concomitantly. Compared with the high-viscosity asphalt, the penetration value of the modified asphalt with a 9% content decreased by 27.2%, the ductility decreased by 43.0%, and the softening point increased by 7.4%. This indicates that the thermal stabilization properties of the high-viscosity bitumen with the addition of nanoscale titanium dioxide have been improved and the resistance unrecoverable deformation ability has been enhanced, but the anti-crack resistance at lower temperatures has decreased and the material's fatigue resilience is weakened.

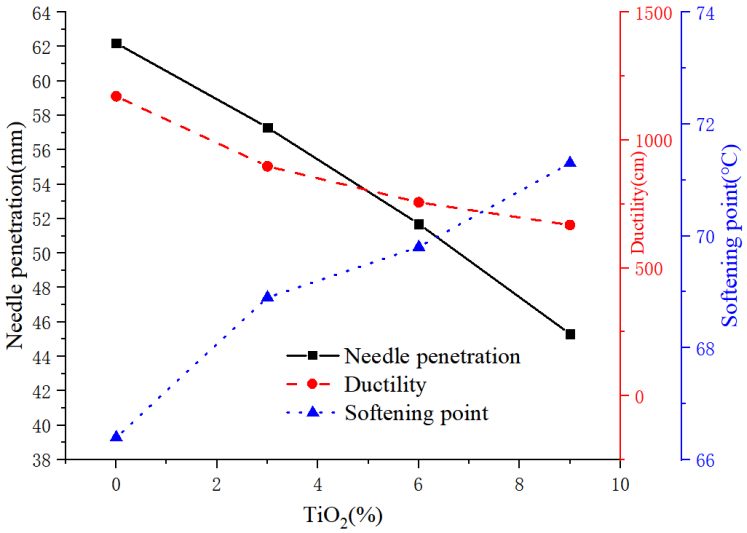


Figure 3. Physical properties of high-viscosity asphalt.

These indicators may not be suitable for evaluating thermal stabilization properties at high temperatures and anti-crack resistance at lower temperatures of the bitumen binder, and cannot simulate the flow deformation of asphalt under continuous loading (such as rutting problems). Therefore, further research on the characteristic of rheology of modified bitumen is needed based on rheological theory.

3.2. Temperature Sweep Tests

Figure 4 shows the complex modulus and phase angle (δ) values for the NHV-modified bitumen when the temperature was between 34 °C and 82 °C. The higher the complex modulus amount, the stiffer the bitumen binder under high temperature or high-frequency load, and the stronger the resistance to rutting. Figure 4 shows that an increase in test temperature results in a gradual decrease in the complex modulus of bitumen. This indicates that temperature has a significant impact on the anti-deformation ability of the bitumen. The modulus of the treated bitumen is gradually increased with the rise in the dosage of nano-TiO_2. As the test temperature rises, the reduction amplitude of the complex modulus of the treated bitumen decreases gradually. It has been discovered that the modulus of the 9% treated bitumen at 34 degrees is 1.40 times that of the high-viscosity asphalt. Nonetheless, the value of the modulus for the 9% bitumen binder at 82 °C is 7.05 times that of the high-viscosity asphalt. This suggests that nano-TiO_2 greatly improves the thermal stability of the binder.

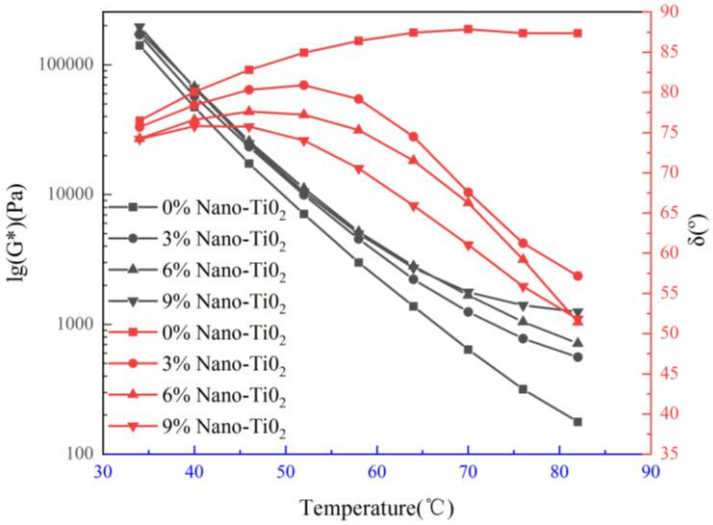


Figure 4. Complex modulus (G*) and phase angle (δ) of NHV-modified bitumen under different test temperatures.

The viscoelastic ratio of asphalt can be obtained by measuring the phase angle. The bitumen binder becomes more elastic and sensitive to cold temperatures at lower phase angles. As can be noted in Figure 4, as the experimental temperature goes up, the phase angle rises steadily, whereas the phase angle of the bitumen binder incorporating nano-TiO_2 initially rises and then falls. Moreover, as the dosage increases, the phase angle of the bitumen binder decreases gradually. This result further suggests that adding nano-TiO_2 reduces bitumen binder sensitivity and improves its elastic properties.

The higher the rutting factor, the better the bitumen binder is at resisting unrecoverable deformation at high temperatures. As seen in Figure 5, the rutting factor decreased across the overall temperature range. The bitumen binder was found to be more susceptible to high-temperature deformation that could not be recovered. The rutting factor of nano titanium dioxide high-viscosity modified asphalt increases with the dosage, under the same temperature conditions, demonstrating that nano-TiO_2 enhances the high-temperature stability of the bitumen binder. The bitumen binder was more prone to high-temperature unrecoverable deformation.

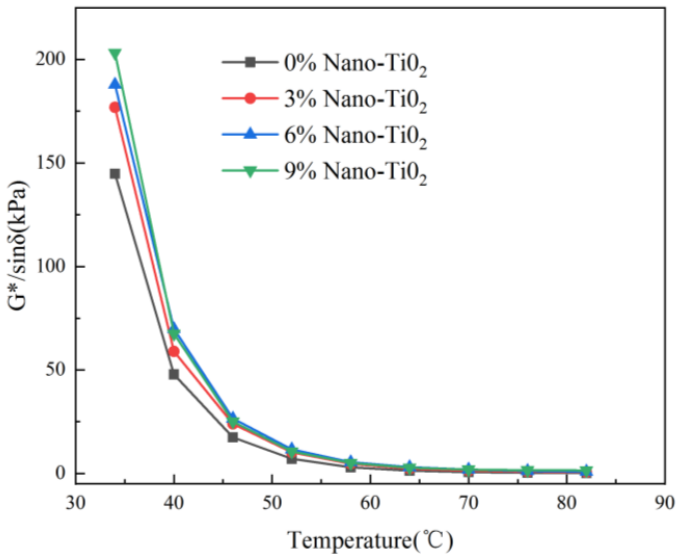


Figure 5. Relationship of rutting factor (G*/sinδ) and test temperature of NHV-modified bitumen.

3.3. Frequency Sweep Test

Figure 6 presents the relation between modulus and frequency in the frequency scanning tests. The dots of different colors in the figure represent the results of the frequency scanning test, and the lines of different colors are the fitting straight lines of the test results.

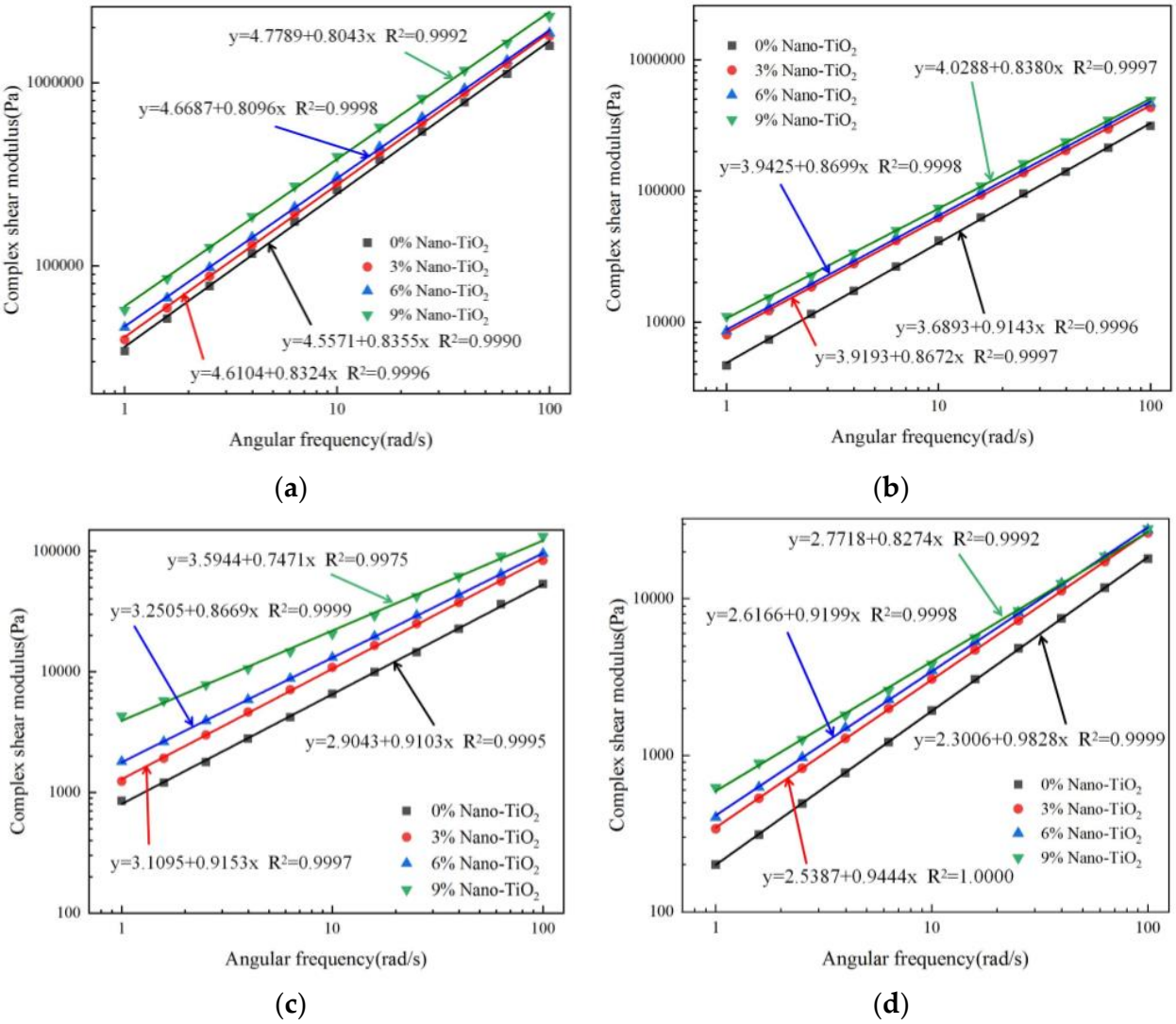


Figure 6. The relationship of the complex shear modulus and the angular frequency: (**a**) 30 °C; (**b**) 40 °C; (**c**) 50 °C; (**d**) 60 °C.

Generally speaking, the high-frequency region can assess the response of pavement under rapid loads, while materials' long-term stability, creep or relaxation characteristics can be reflected in the low-frequency region. With an increase in experimental temperature, the modulus of the bitumen binder decreases in the entire frequency domain, indicating that the temperature sensitivity of the asphalt binder is still very high. Under the condition of 10 rad/w, and at temperatures of 30 degrees and 60 degrees, the modulus of 9% NHV-modified bitumen is 1.52 times that of high-viscosity asphalt and 1.97 times that of high-viscosity asphalt. It suggests that adding nano-TiO_2 significantly enhances the thermal tolerance of the bitumen binder at high temperatures, which is aligned with the findings shown in Figures 4 and 5. With the increase in angular frequency, the modulus gradually increases, and the increased amplitude of the complex shear modulus becomes larger and larger with the increased frequency. Under the test temperature of 60 degrees and the conditions of 100 rad/w, the complex shear modulus of the NHV-modified bitu-

men increased by 8327.9, 9573.4, and 10045.9 Pa, respectively. It indicates that the modified bitumen mixed with nano-TiO_2 demonstrates more excellent performance against impact loads under high-temperature conditions. The modulus has a strong negative linear relationship to the angular frequency in the logarithmic coordinate system, and the lowest determination coefficient of the linear fitting analysis is 0.9975.

3.4. Multi-Stress Creep Recovery (MSCR) Test

3.4.1. Burgers Model

The Burgers model is widely used in viscoelastic mechanics. It is a four-element model (Figure 7). It was used to calculate material parameters and analyze the mechanical characteristics of viscoelastic bitumen binder material [24,25] and the mixture microstructure [26,27]. This model can better characterize the creep deformation characteristics of viscoelastic materials, and its creep compliance is as follows:

$$J(t) = \frac{1}{E_1} + \frac{t}{\eta_2} + \frac{1}{E_2}(1 - e^{-E_2 \times t/\eta_1}) \quad (1)$$

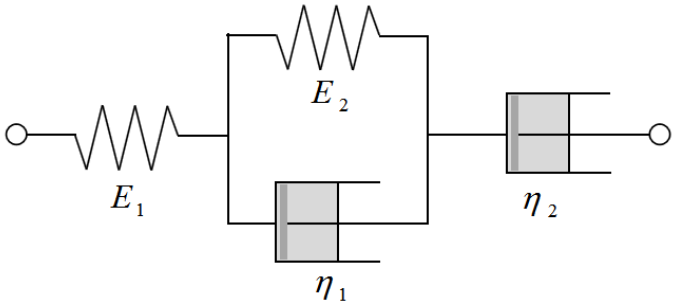


Figure 7. Burgers model diagram.

In the equation above, $J(t)$ is creep compliance of t time, Pa^{-1}; E_1 and E_2 are the spring elastic modulus of the Maxwell and Kelvin model, Pa; η_1 and η_2 are the viscosity parameters of the Kelvin and Maxwell model, $Pa \cdot s$; and t is the time parameter, s.

3.4.2. Fractional Derivative Empirical Creep Model

Various engineering fields have used the FDEC model because it can overcome the shortcoming that the classical integer derivative model and experimental results are not in good agreement [28–31].

The Riemann–Liouville fractional derivative operator is defined as follows [32–34]:

$$(D_{0^+}^{\gamma} f)(t) = \frac{1}{\Gamma(1-\gamma)} \frac{d}{dt} \int_0^t \frac{f(\tau)}{(t-\tau)^{\gamma}} d\tau \; 0 \le \gamma \le 1 \quad (2)$$

When $s = t - \tau$, Equation (3) can be converted into an integral form, as shown below:

$$(D_{0^+}^{\gamma} f)(t) = \frac{1}{\Gamma(1+\gamma) t^{\gamma}} * df \quad (3)$$

The following is an expression of the Abel adhesive pot element [35]:

$$\sigma = \eta I_{\gamma}(t) * d\varepsilon \quad (4)$$

Its creep compliance is as follows:

$$J(t) = \frac{1}{\eta}\varphi(t) * \frac{t^{\gamma-}}{\Gamma(\gamma)} = \frac{1}{\eta\Gamma(\gamma+1)}t^{\gamma} \tag{5}$$

In this expression, $\phi(t)$ is unit strain and $\phi(t) = \begin{cases} 1, t \geq 0 \\ 0, t < 0 \end{cases}$.

The fractional derivative is equivalent to the convolution of the $I_r(t)$.

The Nutting function [36] is the basis for creep behavior in viscoelastic materials, which is shown below:

$$\varepsilon(t) = \lambda t^{\gamma}\sigma,\ 0 < \gamma < 1 \tag{6}$$

Its creep compliance is as follows:

$$J(t) = \lambda t^{\gamma},\ 0 < \gamma < 1 \tag{7}$$

The creep flexibility can be expressed as a power function as demonstrated in Equations (5) and (7).

$$\lambda = \frac{1}{\eta\Gamma(\gamma+1)} \tag{8}$$

The coefficient of viscoelastic material and the order have an effect on λ, as indicated by Formula (8).

3.4.3. Model Fitting Analysis

To maintain data stability and analysis reliability, only the test results from the 29th creep recovery cycle were selected for analysis. The parameter determination method of the Burgers model adopts the fixed parameter fitting method. The remaining parameters are calculated by nonlinear fitting regression analysis. The parameters of the Burgers model and fractional derivative empirical creep model are also obtained by matching the experimental data, as depicted in Figures 8–11. The parameters values of the model obtained through the fitting analysis of data are presented in Figures 12 and 13.

With the gradual increase in nano-TiO_2 content, the deformation behavior of nano-TiO_2-modified bitumen at high temperatures is significantly enhanced, as shown in Figures 8–11. At 60 °C, the initial deformation of 3%, 6%, and 9% modified asphalt is reduced by 22.2%, 47.5%, and 54.4%, respectively, compared with the matrix asphalt.

Both the FDEC and the Burgers models can fit the creep deformation of nano-TiO_2 high-viscosity modified asphalt well, but the smallest R^2 value after adjusting the fitting curve of the Burgers model is 0.9471. The smallest R^2 value after adjusting the fitting curve of the FDEC model is 0.9992. The accuracy of the fit of the FDEC model is higher, and it has fewer parameters. Therefore, the FDEC model has the benefits of fewer parameters and higher fitting accuracy, and it has important theoretical value.

These two models have a certain regularity and physical significance to the fitting parameters of the experimental results. The values of E_2, η_1 and η_2 in the Burgers model gradually decline as the experimental temperature increases, while λ parameters in the fractional derivative empirical model gradually increase. The correlation between the fitting parameters of the two models is shown in Figures 14 and 15. When $p < 0.05$ in the correlation heat map, it is marked as *, as shown in Figure 14. The parameters between the two models have a negative correlation. Among them, in the logarithmic coordinate system, the correlation between parameters η_1, η_2, and λ indicates that the λ parameter can assess the ability of the modified bitumen to resist deformation. That is, the bigger the λ, the superior the resistance to deformation of the bitumen binder. It further explains that the parameters of the FDEC model have certain physical significance.

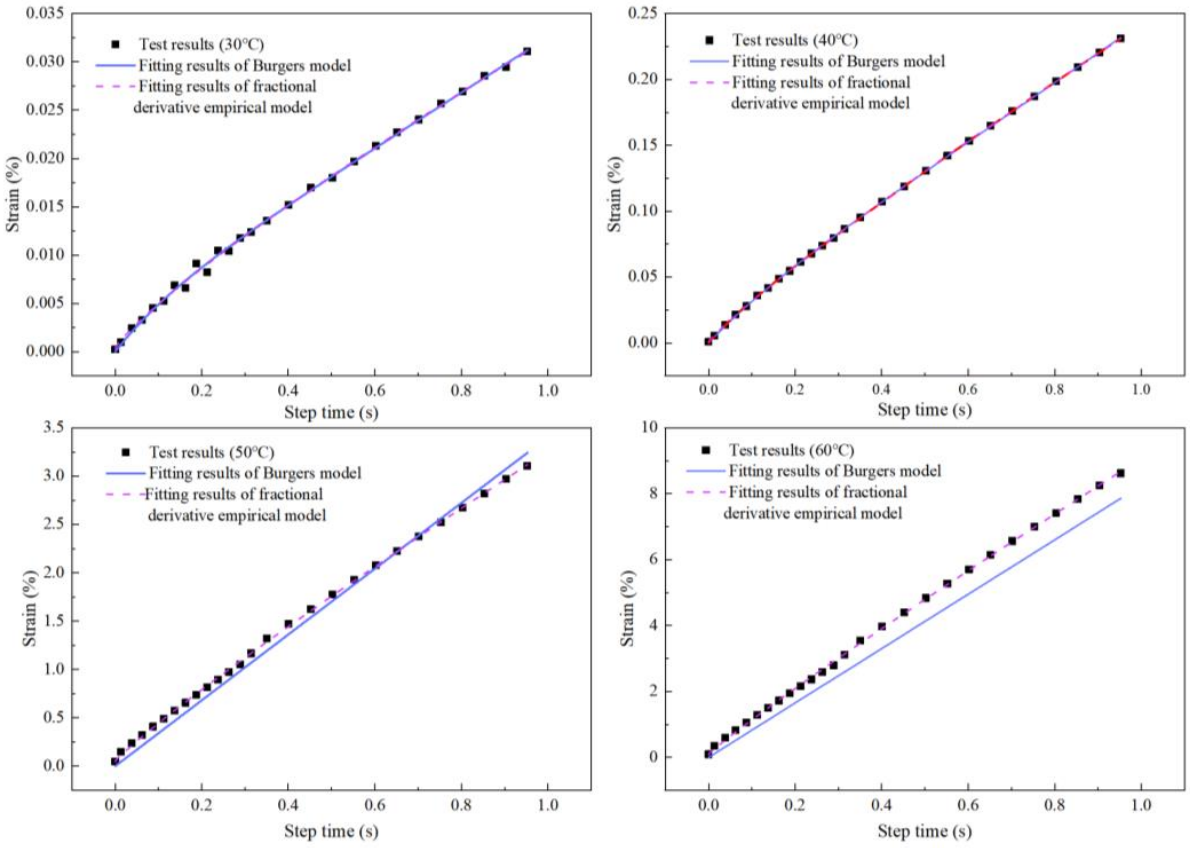


Figure 8. Test results and fitting curves (high-viscosity asphalt).

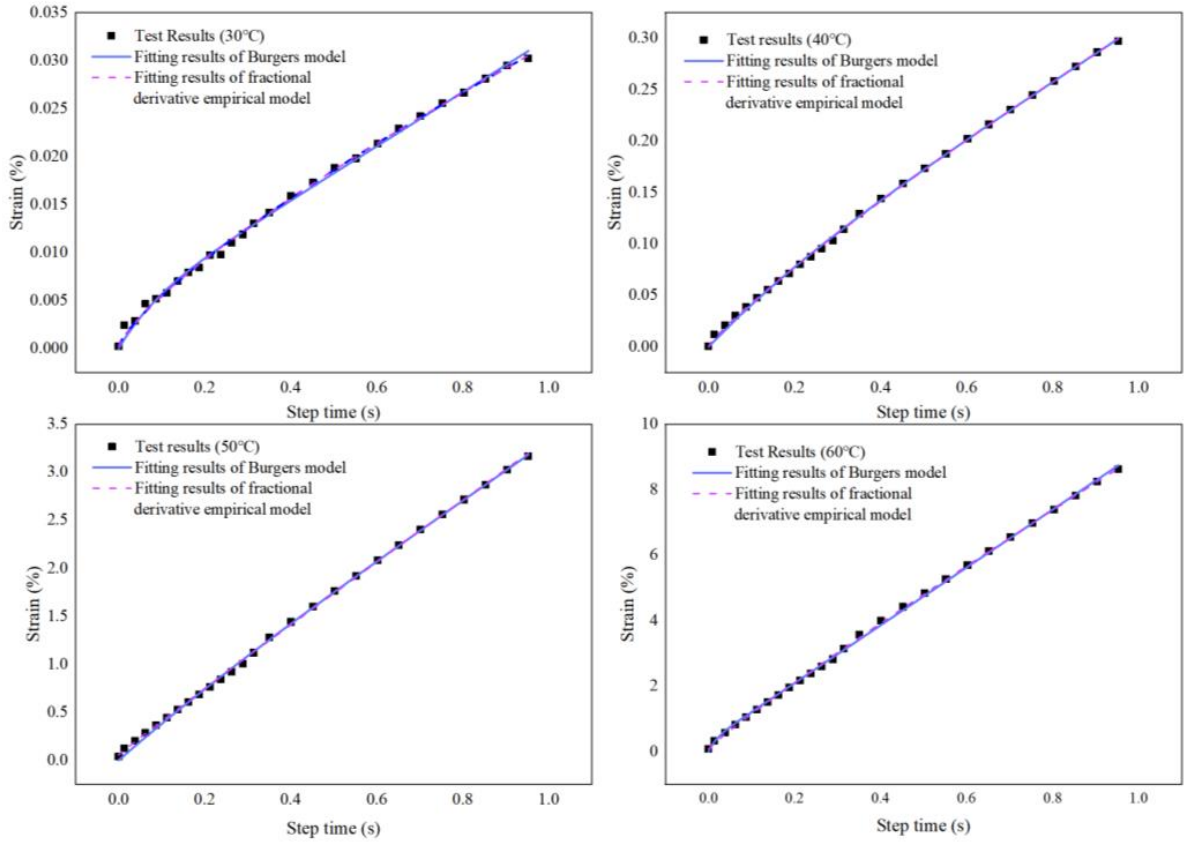


Figure 9. Test results and fitting curves (modified asphalt with 3% nano-TiO_2).

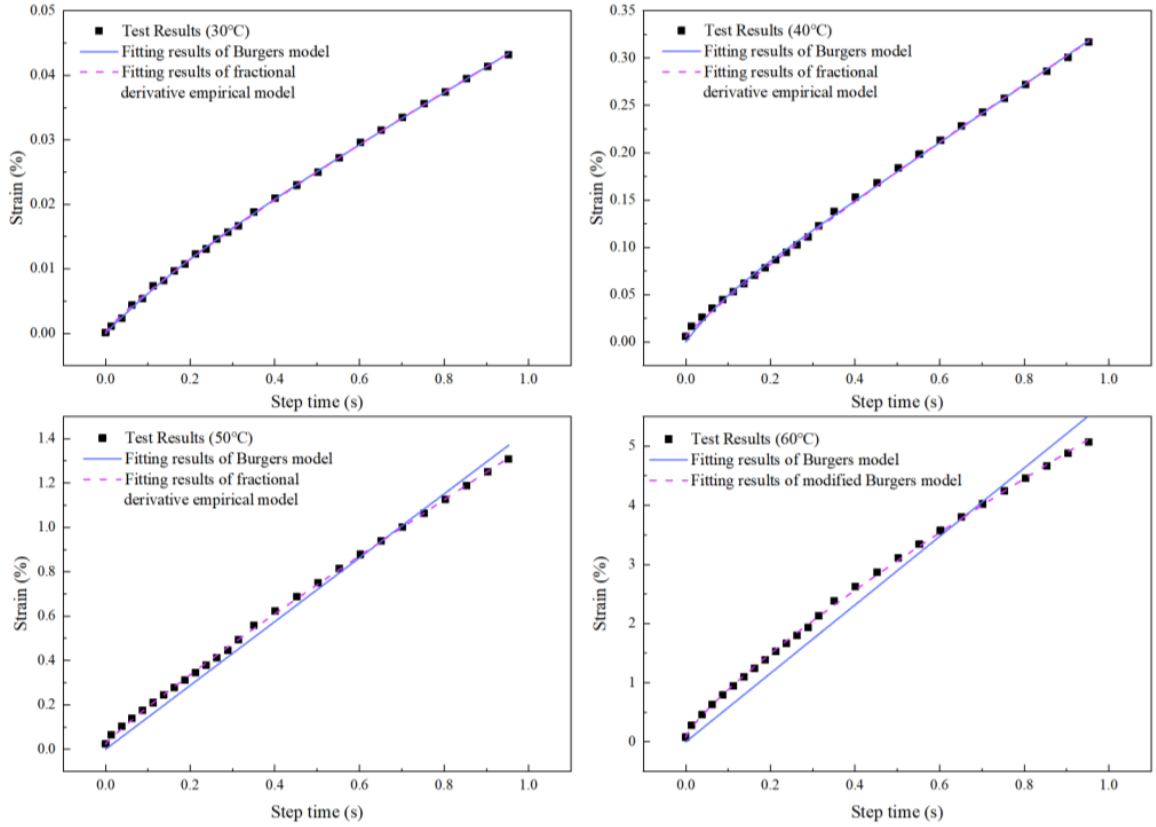


Figure 10. Test results and fitting curves (modified asphalt with 6% nano-TiO_2).

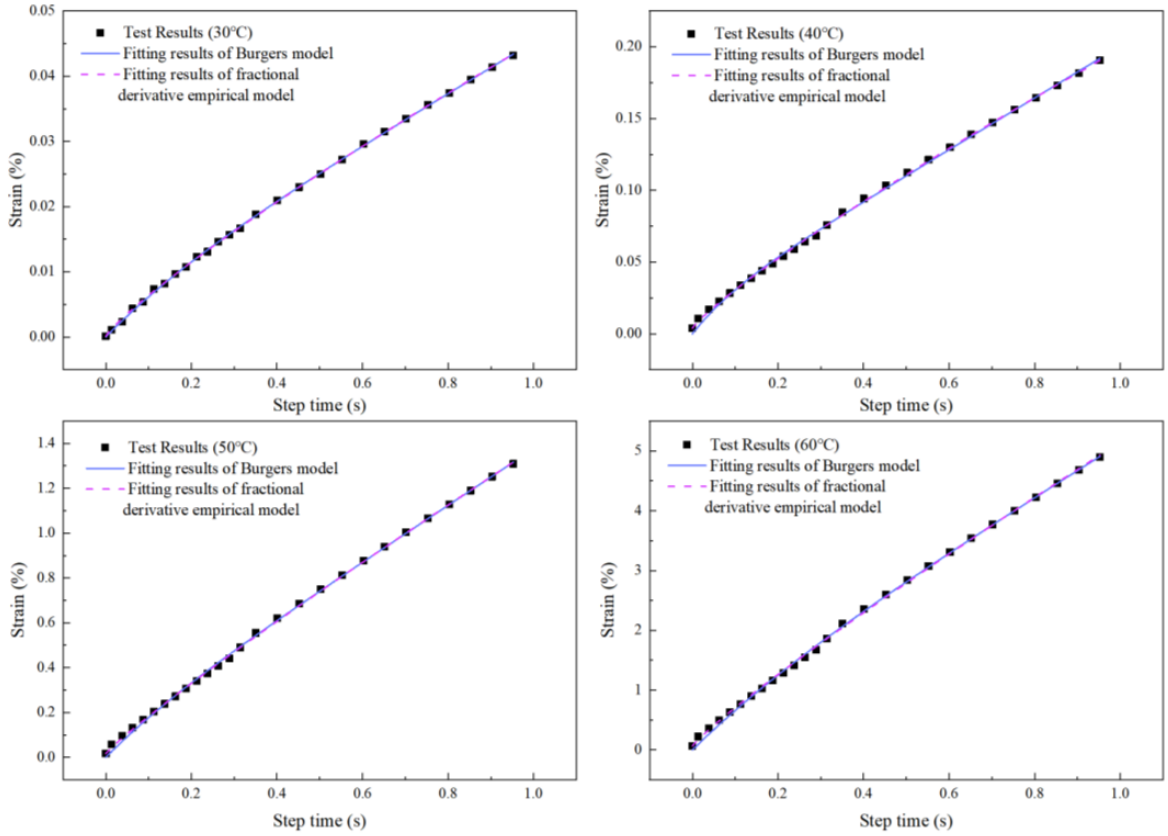


Figure 11. Test results and fitting curves (modified asphalt with 9% nano-TiO_2).

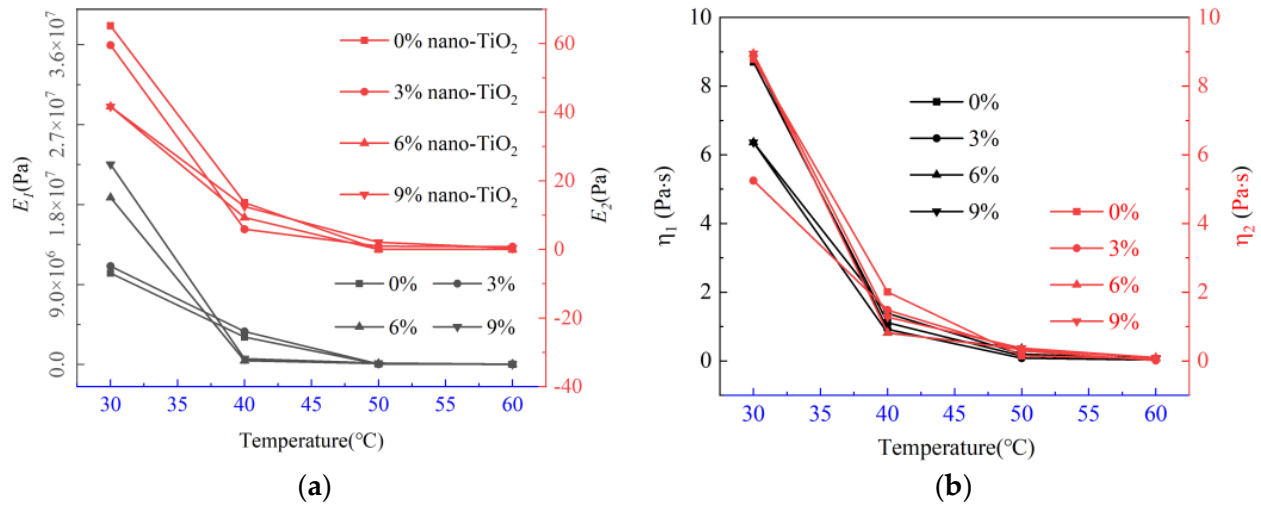


Figure 12. The parameter values of the Burgers model: (**a**) E_1 and E_2; (**b**) η_1 and η_2.

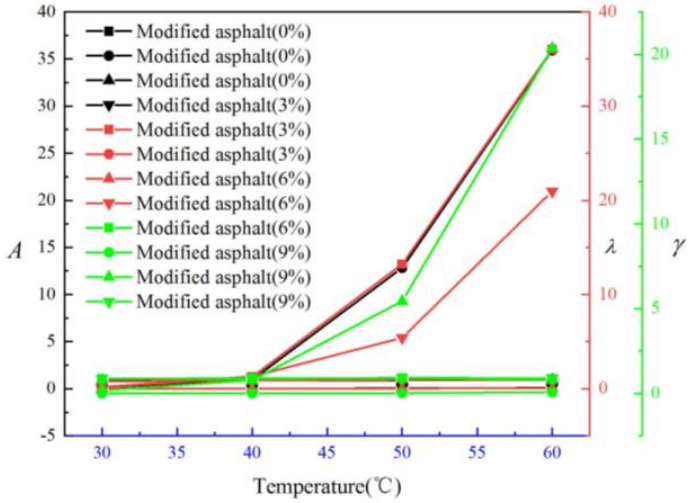


Figure 13. The parameter values of the FDEC model.

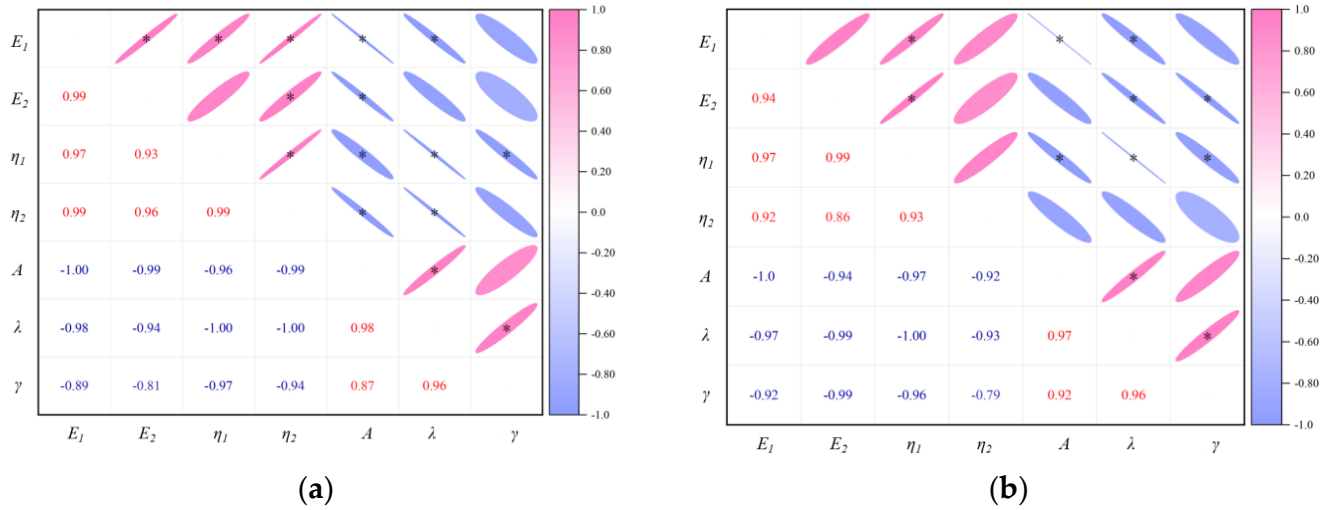


Figure 14. *Cont.*

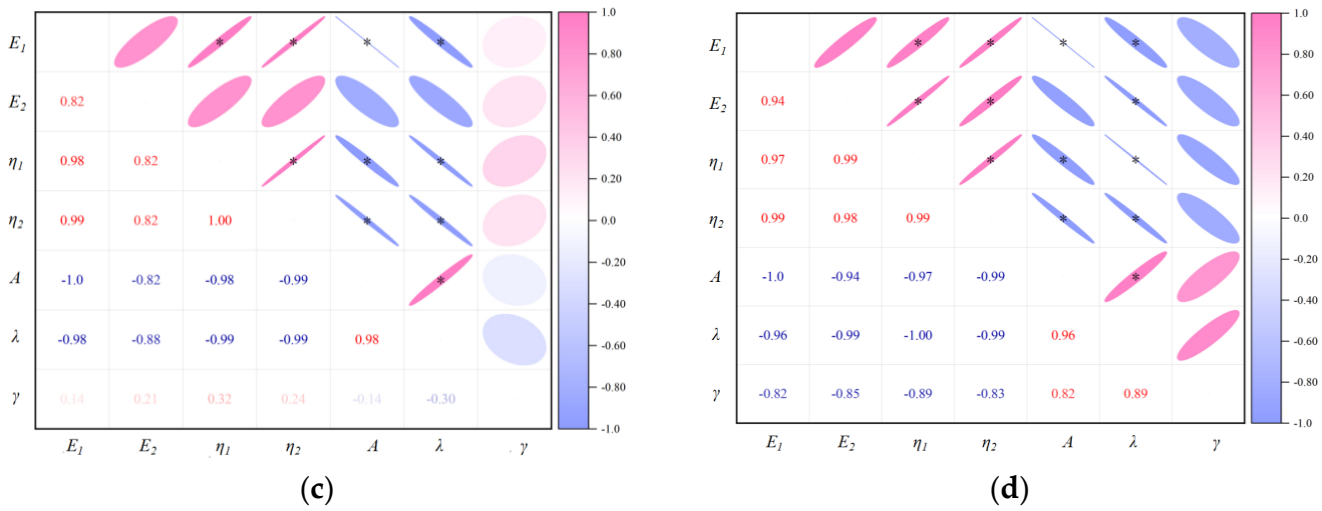


Figure 14. Correlation diagram of model fitting parameters: (**a**) high-viscosity asphalt; (**b**) modified asphalt (3%); (**c**) modified asphalt (6%); (**d**) modified asphalt (9%).

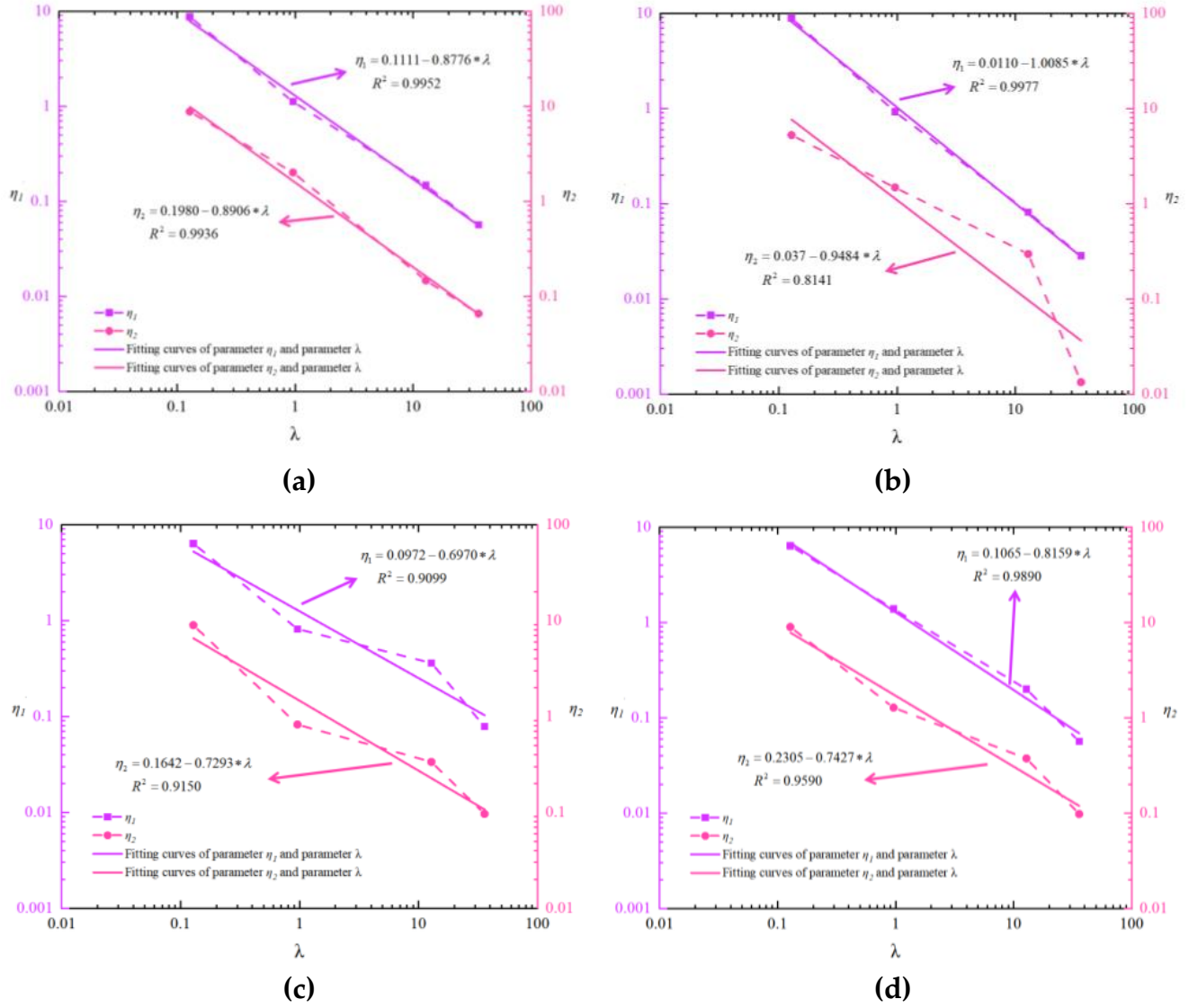


Figure 15. The correlation between parameters η_1, η_2 and λ: (**a**) high-viscosity asphalt; (**b**) modified asphalt (3%); (**c**) modified asphalt (6%); (**d**) modified asphalt (9%).

3.5. Bending Creep Stiffness Test

The greater the creep stiffness is, the lower the capability of the NHV-modified bitumen to protect against the risk of deforming at lower temperatures, and it is more likely to crack in cold conditions. The m value represents the temperature sensitivity of the material. The smaller the m, the higher the temperature sensitivity, as Figures 16 and 17 show. As the dosage of nano-TiO_2 increases, the creep stiffness steadily grows under the constant temperature environment. It indicates that using nano titanium dioxide made the modified bitumen more crisp and likely to crack at lower temperatures. When the experimental temperature drops, the bitumen stiffness rises gradually, indicating that with the decrease in temperature, the crack resistance performance of the asphalt binder further decreases. Moreover, the lower the temperature and the larger dosage of nano titanium dioxide, the worse the crack resistance of the bitumen binder. Under the condition of −18 °C, the creep stiffness of 9% NHV-modified asphalt is 9.39 times that of high-viscosity asphalt.

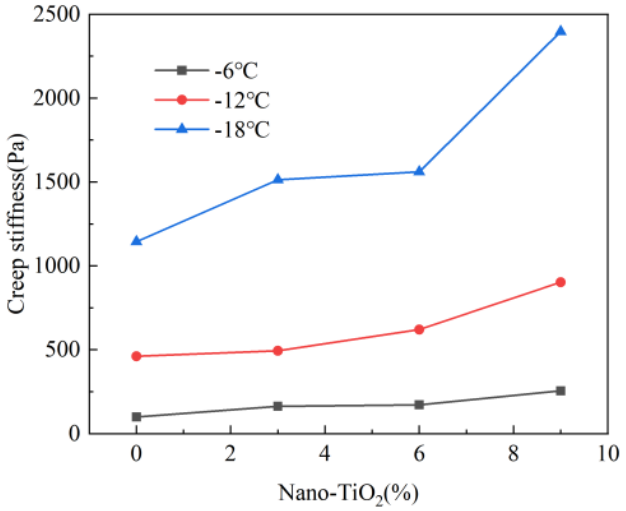


Figure 16. Creep stiffness value.

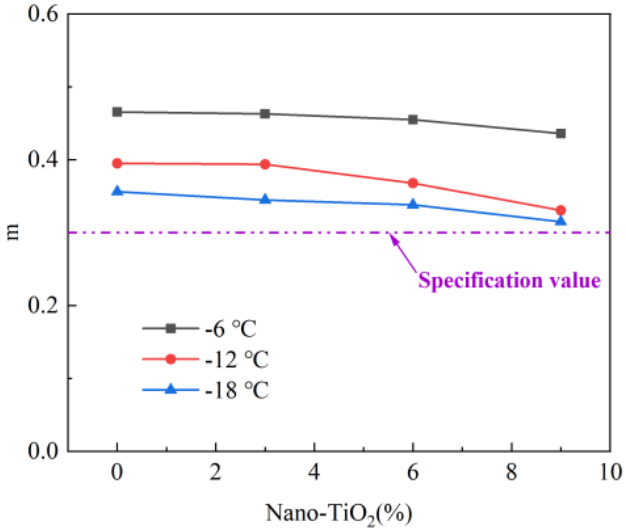


Figure 17. m value.

The m values of 3%, 6%, and 9% nano-TiO_2-modified asphalt at different temperatures are all greater than 0.3. This indicates that although the characteristics at low temperatures of nano titanium dioxide high-viscosity modified bitumen decrease with the increase in modifier dosage, the low-temperature performance of 3%, 6%, and 9% nano-TiO_2-

modified bitumen meets the specification requirements [15]. However, the m value of 9% nano-TiO_2 high-viscosity modified bitumen at −18 °C is very close to the specification value, so the dosage of nano titanium dioxide should be reduced. Therefore, considering that thermal stability behavior of nano-TiO_2 high-viscosity modified bitumen improves with a higher nano-TiO_2 content, 6% is recommended as the optimal content.

3.6. Long-Term Aging Performance

According to Section 2.2.6, the residual penetration ratio (RPR) and softening point increment (SPI) of nano-TiO_2-modified high-viscosity bitumen after prolonged aging were conducted for investing prolonged aging characteristics. This is clear from Figure 18.

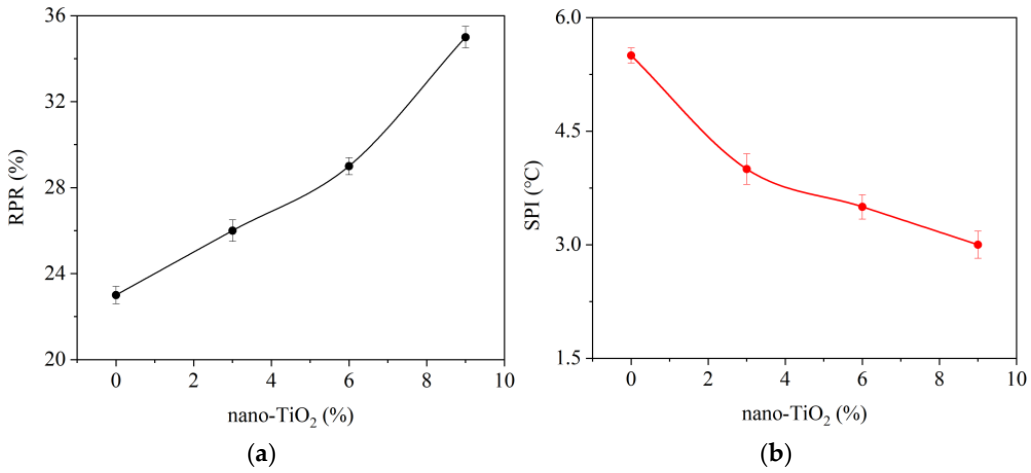


Figure 18. (**a**) RPR of nano-TiO_2-modified asphalt; (**b**) SPI of nano titanium dioxide-modified bitumen.

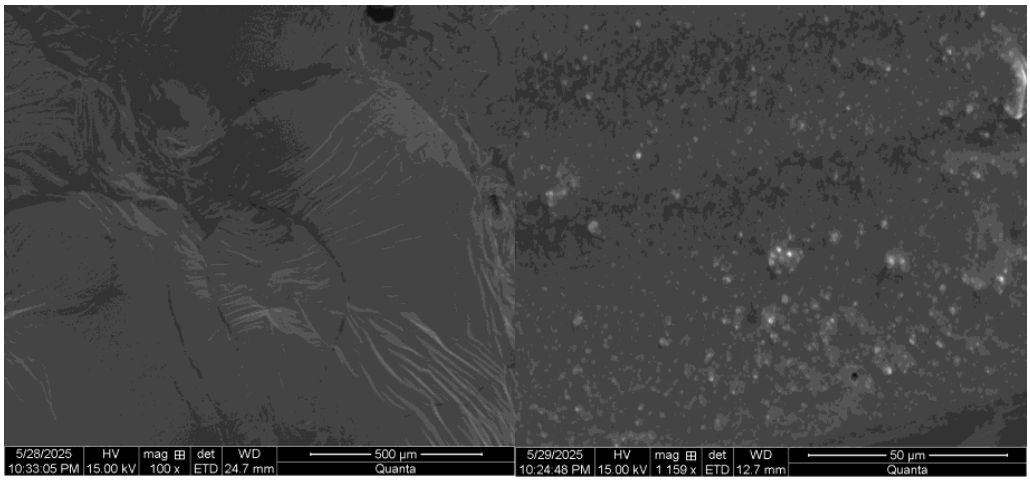
The RPR of nano-TiO_2 high-viscosity modified bitumen increases as the nano-TiO_2 content increases, as shown in Figure 18a. Compared with original bitumen, the RPR of nano titanium dioxide-modified bitumen containing 3%, 6% or 9% of nano-TiO_2 increases by 13%, 24% or 52%, respectively. The prolonged resistance of bitumen binder to aging is enhanced by the rise in nano titanium dioxide content. It is because the added nano-TiO_2 absorbs external energy, and the hardening rate of asphalt under the impact of hot oxygen and reduced pressure. The prolonged aging resistant properties of bitumen have been improved.

As shown in Figure 18b, the SPI of nano titanium dioxide-modified high-viscosity bitumen falls with an increase in the nano-TiO_2 content. Compared with base asphalt, the SPI of nano-TiO_2-modified asphalt increased by 27%, 50%, and 71% with 3%, 6%, and 9% additions, respectively.. The smaller the SPI of asphalt, the higher its long-term aging performance. It demonstrates that nano-TiO_2 can enhance the aging resistance of asphalt. This is because nano-TiO_2 is distributed in a uniform way throughout the bitumen, and creates a stable structure with asphalt to effectively absorb heat. The oxidation process of asphalt is inhibited, which improves the long-term durability of asphalt.

3.7. Modification Mechanism of Nano-TiO_2-Modified Asphalt

3.7.1. SEM

According to Section 2.2.6, SEM pictures of the original bitumen and nano-TiO_2-modified high-viscosity bitumen were taken to study the fusion state of nano-TiO_2 and asphalt as depicted in Figure 19.



(**a**) (**b**)

Figure 19. SEM image: (**a**) base asphalt; (**b**) nano-TiO_2-modified bitumen.

As shown in Figure 19, the original bitumen interface is smooth and free of impurities. Nano-TiO_2 particles are mainly uniformly distributed in asphalt. This is because nano-TiO_2 has high surface energy and active energy, and can be fully mixed with asphalt under a high-speed shear force, avoiding the occurrence of the agglomeration phenomenon. Therefore, nano-TiO_2 can successfully isolate the impact of ultraviolet light on the bitumen binder, and effectively improve the high-temperature and anti-aging performance of the bitumen binder. In addition, the uniform fusion of nano-TiO_2 and asphalt increases the asphaltene percentage, improving thermal stability and temperature sensitivity.

3.7.2. FTIR

The infrared spectra of the original specimen and nano-TiO_2-modified asphalt were tested according to Section 2.2.7. The interaction between original bitumen and nano-TiO_2 was studied, as shown in Figure 20.

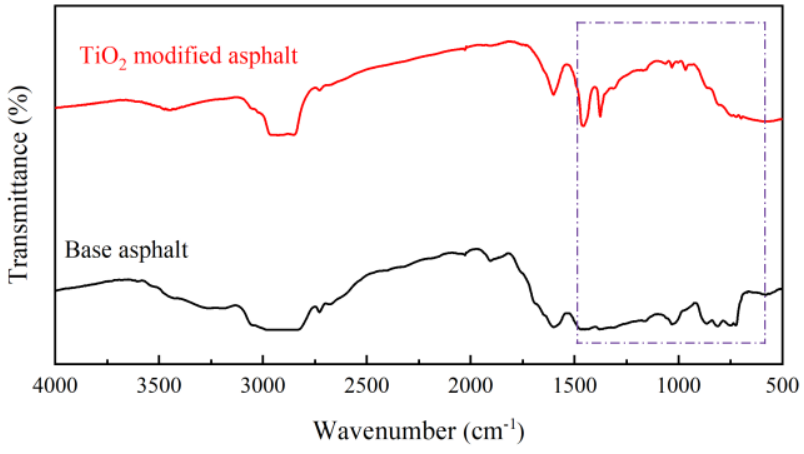


Figure 20. Infrared spectra of base asphalt and nano-TiO_2 high-viscosity modified bitumen.

In comparison to the original bitumen, the characteristic peaks in the infrared spectra of nano-TiO_2-modified high-viscosity bitumen are primarily within 1500 cm^{-1} to 637 cm^{-1}, as shown in the framed area in Figure 20 Specifically, a characteristic peak appears at 914 cm^{-1} in the infrared spectrum, which is the result of the bending vibration of Ti-Ti bonds. Additionally, characteristic peaks observed between 520 cm^{-1} and 470 cm^{-1} arise from the bending vibrations of Ti-O bonds. These observations indicate that the func-

tional groups of TiO_2 nanoparticles are preserved after blending with asphalt, and a nanostructured layer is formed. Furthermore, the peak positions and transmittance values of the spectral curves remain nearly identical. There is no new chemical bond formation. It demonstrates that the nano titanium dioxide-modified bitumen binder undergoes a blending process rather than chemical bonding.

4. Conclusions

(a) The heightened temperature tolerance of the nano-TiO_2 high-viscosity modified asphalt has been improved, the anti-rutting ability has been enhanced, and the crack resistance performance at lower temperature has decreased.

(b) The results of temperature scanning tests and frequency scanning tests show that nano titanium dioxide can significantly improve the heightened temperature tolerance of bitumen binders. The sensitivity of the bitumen binder is reduced, and the elastic characteristics of the bitumen are improved. In the logarithmic coordinate system, the complex shear modulus exhibits an excellent linear correlation with the angular frequency. However, under low-temperature conditions, nano-TiO_2 gradually enhances the creep stiffness of the bitumen binder, indicating that nano-TiO_2 makes the bitumen brittle and more liable to cracking at lower temperatures.

(c) The fitting analysis of the MSCR results of NHV-modified asphalt using the Burgers model and the FDEC model shows that both these two models can fit the creep deformation of nano-TiO_2 high-viscosity modified asphalt well, but the FDEC model has higher accuracy and fewer parameters. The parameters have certain physical meanings, among which λ can represent the ability index of modified asphalt to resist unrecoverable deformation at high temperatures.

(d) In addition to the rheological characteristics of the bitumen binder, critical mechanical characteristic aspects like fatigue life, tensile strength, rutting resistance, and fracture toughness in the field are very important. In future research, these indicators will be thoroughly studied to explore the practical applicability of nano-TiO_2-modified asphalt in real-world pavement design.

Author Contributions: Conceptualization, R.L. and Y.Y.; methodology, R.L. and L.L.; validation, R.L., and Z.W.; formal analysis, R.L.; investigation, S.Z. and Y.M.; writing—original draft preparation, R.L. and L.L.; writing—review and editing, R.L. and L.L. All authors have read and agreed to the published version of the manuscript.

Funding: This research was supported by the science and technology public relations planned project of Henan Province, grant number 252102230140. This project was supported by Open Research Fund Program of Henan Key Laboratory of Engineering Materials and Hydraulic Structures, grant number HNEMHS_OF202402.

Institutional Review Board Statement: Not applicable.

Informed Consent Statement: This research does not involve human beings.

Data Availability Statement: The original contributions presented in this study are included in the article. Further inquiries can be directed to the corresponding author.

Conflicts of Interest: Author Shikang Zhou was employed by China Communications First Highway Group Xiamen Engineering Co., Ltd. Zhigang Wang was employed by Pingdingshan Highway Development Center. The remaining authors declare that the research was conducted in the absence of any commercial or financial relationships that could be construed as a potential conflict of interest.

References

1. Angel, S.; Parent, J.; Civco, D.L.; Blei, A.; Potere, D. The dimensions of global urban expansion: Estimates and projections for all countries, 2000–2050. *Prog. Plan.* **2011**, *75*, 53–107. [CrossRef]
2. Nuruzzaman, M. Urban heat island: Causes, effects and mitigation measures-a review. *Int. J. Environ. Monit. Anal.* **2015**, *3*, 67–73. [CrossRef]
3. Jabbar, H.K.; Hamoodi, M.; Al-Hameedawi, A.N. Urban heat islands: A review of contributing factors, effects and data. *J. 2023 IOP Conf. Ser. Earth Environ. Sci.* **2023**, *1129*, 012038. [CrossRef]
4. Chathuranga, S.; Chandana Jayaratne, K.P.S. A systematic review of urban heat island impact on selected Asian cities. Chandana Jayaratne. *Proc. Tech. Sess.* **2025**, *41*, 87–95.
5. Li, H.; Wang, H.; Lin, J.; Yang, J.; Yao, Y. Study on the Effect of SBS/HVA/CRM Composite-Modified Asphalt on the Performance of Recycled Asphalt Mixtures. *Polymers* **2024**, *16*, 3226. [CrossRef]
6. Xie, T.; He, Z.; Yu, H.; Ma, Y.; Shi, C.; Zhang, C.; Ge, J.; Dai, W. Evaluation of styrene butadiene rubber asphalt modification mechanism and adhesion effect based on molecular simulation. *Fuel* **2024**, *364*, 131023. [CrossRef]
7. Li, E.; Xu, W.; Zhang, Y. Performance study of waste pe-modified high-grade asphalt. *Polymers* **2023**, *15*, 3200. [CrossRef]
8. Ji, H.; He, D.; Li, B.; Lu, G.; Wang, C. Evaluation of rheological and anti-aging properties of TPU/Nano-TiO_2 composite-modified asphalt binder. *Materials* **2022**, *15*, 3000. [CrossRef] [PubMed]
9. Xie, Y.; Yu, P.; Zhai, M. Analysis of Nano-ZnO-modified asphalt compatibility based on molecular dynamics. *Materials* **2023**, *16*, 4710. [CrossRef]
10. Kyriakodis, G.-E.; Santamouris, M. Using reflective pavements to mitigate urban heat island in warm climates-results from a large scale urban mitigation project. *Urban Clim.* **2018**, *24*, 326–339. [CrossRef]
11. Sha, A.; Liu, Z.; Tang, K.; Li, P. Solar heating reflective coating layer (SHRCL) to cool the asphalt pavement surface. *Constr. Build. Mater.* **2017**, *139*, 355–364. [CrossRef]
12. Singh, H.; Thind, P.S.; Singh, S.; John, S. Applicability of TiO_2-Laden asphalt pavements in reducing the vehicular pollution of chandigarh, India. *Clean-Soil Air Water* **2022**, *50*, 5. [CrossRef]
13. Carneiro, J.O.; Azevedo, S.; Teixeira, V.; Fernandes, F.; Freitas, E.; Silva, H.; Oliveira, J. Development of photocatalytic asphalt mixtures by the deposition and volumetric incorporation of TiO_2 nanoparticles. *Constr. Build. Mater.* **2013**, *38*, 594–601. [CrossRef]
14. Xu, X.; Wei, L.; Chen, J.; Rong, H. Physical, rheological and micro characteristics of ARA/Nano-TiO_2 composite modified asphalt before and after short-term aging. *Mater. Today Commun.* **2024**, *39*, 109097. [CrossRef]
15. Enieb, M.; Cengizhan, A.; Karahancer, S.; Eltwati, A. Evaluation of physical-rheological properties of nano titanium dioxide modified asphalt binder and rutting resistance of modified mixture. *Int. J. Pavement Res. Technol.* **2023**, *16*, 285–303. [CrossRef]
16. Diniz, M.I.L.; Lucena, A.E.d.F.L.; Neto, O.d.M.M.; Moraes, T.M.R.P.d.; Sousa, T.M.d.; Silva, I.M.; F'elix, C.T.R. Titanium dioxide as a modifier in asphalt mixtures: Mechanical behavior under aging conditions. *Constr. Build. Mater.* **2025**, *461*, 139816. [CrossRef]
17. Chen, Z.; Zhang, D.; Zhang, Y.; Zhang, H.; Zhang, S. Influence of multi-dimensional nanomaterials composite form on thermal and ultraviolet oxidation aging resistances of SBS modified asphalt. *Constr. Build. Mater.* **2021**, *273*, 122054. [CrossRef]
18. Lima, O.; Afonso, C.; Segundo, I.; Landi, S., Jr.; Homem, N.; Freitas, E.; Alcantara, A.; Branco, V.; Soares, S.; Soares, J.; et al. Aging evaluation of an asphalt binder modified by nano-TiO_2. *Nanomaterials* **2022**, *12*, 1678. [CrossRef]
19. Zheng, D.; Qian, Z.; Li, P.; Wang, L. Performance evaluation of high-elasticity asphalt mixture containing inorganic nano-titanium dioxide for applications in high altitude regions. *Constr. Build. Mater.* **2019**, *199*, 594–600. [CrossRef]
20. *JTG E20-2011*; Standard Test Methods of Bitumen and Bituminous Mixtures for Highway Engineering. China Communications Press: Beijing, China, 2011.
21. Bahia, H.; Hanson, D.; Zeng, M.; Zhai, H.; Khatri, M.; Anderson, R. NCHRP REPORT 459: Characterization of Modified Asphalt Binders in Superpave Mix Design. 2001. Available online: https://onlinepubs.trb.org/Onlinepubs/nchrp/nchrp_rpt_459-a.pdf (accessed on 10 May 2025).
22. Yang, Q.; Liu, Q.; Zhong, J.; Hong, B.; Wang, D.; Oeser, M. Rheological and micro-structural characterization of bitumen modified with carbon nanomaterials. *Constr. Build. Mater.* **2019**, *201*, 580–589. [CrossRef]
23. Zhang, L.; Xing, C.; Gao, F.; Li, T.; Tan, Y. Using DSR and MSCR tests to characterize high temperature performance of different rubber modified asphalt. *Constr. Build. Mater.* **2016**, *127*, 466–474. [CrossRef]
24. Lv, M.; Li, H.; Zhang, S.; Liu, W.; Zhang, H.; Lin, H.; Sun, M. Evolution of rheological and microscopic properties of asphalt binders under fuel corrosion. *Processes* **2024**, *12*, 403. [CrossRef]
25. *AASHTO T 313-22—Determining the Flexural Creep Stiffness of Asphalt Binder Using the Bending Beam Rheometer (BBR)*; AASHTO: Washington, DC, USA, 2022.
26. Yang, J.; Xu, G.; Kong, P.; Chen, X. Characterization of desulfurized crumb rubber/styrene-butadiene-styrene composite modified asphalt based on rheological properties. *Materials* **2021**, *14*, 3780. [CrossRef]

27. Wang, J.; Xue, Z.; Guo, M.; Zhang, S. Using the Rheological Index to Quantitatively Evaluate the Mechanical Performance of High-Elasticity Modified Asphalt. *Adv. Mater. Sci. Eng.* **2021**, 6614644. [CrossRef]
28. Zhang, Y.; Liu, X.; Yin, B.; Luo, W. A nonlinear fractional viscoelastic-plastic creep model of asphalt mixture. *Polymers* **2021**, *13*, 1278. [CrossRef]
29. Klimczak, M. Viscoelastic analysis of asphalt concrete with a digitally reconstructed microstructure. *Materials* **2024**, *17*, 2443. [CrossRef]
30. Makris1, N.; Constantinou, M.C. Fractional-derivative Maxwell model for viscous dampers. *J. Struct. Eng.* **1991**, *117*, 2708–2724. [CrossRef]
31. Sasso, M.; Palmieri, G.; Amodio, D. Application of fractional derivative models in linear viscoelastic problems mech time-depend Mater. *Mech. Time-Depend. Mater.* **2011**, *15*, 367–387.
32. Brociek, R.; Hetmaniok, E.; Słota, D. Numerical solution for the heat conduction model with a fractional derivative and temperature-dependent parameters. *Symmetry* **2024**, *16*, 667. [CrossRef]
33. Riaz, M.; Khan, Z.A.; Ahmad, S.; Ateya, A.A. Fractional-order dynamics in epidemic disease modeling with advanced perspectives of fractional calculus. *Fractal Fract.* **2024**, *8*, 291. [CrossRef]
34. Samko, S.G.; Kilbas, A.A.; Marichev, O.L. *Fractional Integrals and Derivatives: Theory and Applications*; Gordon and Breach: Amsterdam, The Netherlands, 1993.
35. Podlubny, I. *Fractional Differential Equations*; Academic Press: San Diego, CA, USA, 1999.
36. Kilbas, A.A.; Srivastava, H.M.; Trujillo, J.J. *Theory and Applications of Fractional Differential Equations (North Holland Mathematics Studies)*; Elsevier: Amsterdam, The Netherlands, 2006.

Disclaimer/Publisher's Note: The statements, opinions and data contained in all publications are solely those of the individual author(s) and contributor(s) and not of MDPI and/or the editor(s). MDPI and/or the editor(s) disclaim responsibility for any injury to people or property resulting from any ideas, methods, instructions or products referred to in the content.